CHIN. PHYS. LETT. Vol. 33, No. 3 (2016) 037302

Tunneling Negative Magnetoresistance via δ Doping in a Graphene-Based Magnetic Tunnel Junction *

Jian-Hui Yuan(袁建辉)[1]**, Ni Chen(陈妮)[1], Hua Mo(莫华)[1], Yan Zhang(张燕)[1], Zhi-Hai Zhang(张志海)[2]**

[1]*Department of Physics, Guangxi Medical University, Nanning 530021*

[2]*School of Physics and Electronics, Yancheng Teachers University, Yancheng 224051*

(Received 23 October 2015)

We investigate the tunneling magnetoresistance via δ doping in a graphene-based magnetic tunnel junction in detail. It is found that the transmission probability and the conductance oscillates with the position and the aptitude of the δ doping. Also, both the transmission probability and the conductance at the parallel configuration are suppressed by the magnetic field more obviously than that at the antiparallel configuration, which implies a large negative magnetoresistance for this device. The results show that the negative magnetoresistance of over 300% at $B = 1.0$ T is observed by choosing suitable doped parameters, and the temperature plays an important role in the magnetoresistance. Thus it is possible to open a way to effectively manipulate the magnetoresistance devices, and to make a type of magnetoresistance device by controlling the structural parameter of the δ doping.

PACS: 73.23.−b, 03.65.Pm, 73.43.Cd, 75.70.Ak DOI: 10.1088/0256-307X/33/3/037302

Graphene is a single two-dimensional array of carbon atoms with a honeycomb lattice.[1] In the absence of doping, the electronic band structure of graphene consists of two inequivalent pairs of cones (K, K') located at Brillouin-zone corners.[2] In the vicinity of the two inequivalent pairs of cones, charge carriers in a wide single-layer graphene behave like relativistic chiral massless particles with a value of the Fermi velocity ($v_{\rm F} \simeq 1 \times 10^6$ m/s).[2] Such Dirac-like quasiparticles can be described directly by the two-dimensional (2D) Dirac–Weyl equation.[1,2] Thus it is expected to induce some unusual electronic transport properties, which are very different from the two-dimensional electronic gas. As a result, it is hopeful that these peculiar phenomena can be used to develop the relativistic electronic devices.

Recently, a simple method has been developed for the growth of graphene films in a large scale by using chemical vapor deposition (CVD).[3,4] This is a quite important means for the future design of graphene-based devices. For example, a gate-tunable linear magnetoresistance (MR) of ∼600% at 12 T has been reported in metal-shunted devices fabricated on CVD grown graphene.[5] In experiment, magnetic field dependence of the barrier (magnetic barrier) technology has already been employed to create the graphene heterostructure. In particular, the magnetic field modulation electronic transport in graphene has been reported in structures involving one or several magnetic barriers[6−9] as well as superlattices,[10−14] such as the MR effect, spin current and spin polarization, wave vector filter and spin-switching effect. MR is of great interest for device applications due to the fact that it enables more sensitive detection at a smaller scale. Recent experiments on the graphene-based magnetic tunnel junction have shown a large MR, spin and charge transport.[15−18] Friedman *et al.* reported a linear MR in multilayer epitaxial graphene grown on SiC and found that the multilayer epitaxial graphene exhibits large linear MR from 2.2 K up to room temperature which can be best explained by a purely quantum mechanical model.[19] A giant negative magnetoresistance of up to 28% at 2.5 T is observed in plasma-hydrogenated graphene at 2.0 K by Matis *et al.*[20]

In this Letter, we study the tunneling MR via δ doping in a graphene-based magnetic tunnel junction (GMTJ). As shown in Fig. 1, the profile of a magnetic field in the δ-like form is used, which can be produced by using ferromagnetic electrodes deposited on the graphene layer, experimentally.[10,21] A controlling δ-doping potential is exerted on the GMTJ, which can be realized by doping a narrow electric barrier into this nanostructure by the atomic dimensional-control techniques.[22−25] So far, such a system has not been well reported.

We consider a graphene layer in perpendicular magnetic fields as delta functions,[10,26−29]

$$\boldsymbol{B}(x) = B(\delta(x) - \eta\delta(x - D))\hat{z},$$

where the typical value $D = 100$ nm,[27] $\eta = -1$ and $+1$ correspond to the direction of magnetic field in parallel (P) and in antiparallel (AP) with the configuration, respectively. This profile of the magnetic field induces the step-like vector potential as shown in Fig. 1.

$$A_y(x) = B\ell_B(\Theta(x) - \eta\Theta(x - D)),$$

where $\ell_B = \sqrt{\hbar/eB_0} = 813$ Å is a length scale with a typical magnetic field strength $B_0 = 0.1$ T.[27] In the presence of perpendicular magnetic field $B(x)$ and taking into account the δ-doping, the Hamiltonian describing each such point is

$$H = v_{\rm F}\boldsymbol{\sigma} \cdot (\boldsymbol{p} + e\boldsymbol{A})) + \gamma_0\delta(x - x_0), \qquad (1)$$

*Supported by the National Natural Science Foundation of China under Grant Nos 11447101 and 11447193, the Youth Science Foundation of Guangxi Medical University of China under Grant No GXMUYSF201313, and the Guangxi Department of Education Research Projects of China under Grant No KY2015LX046.

**Corresponding authors. Email: jianhui831110@163.com; zhangzhihai3344@163.com

© 2016 Chinese Physical Society and IOP Publishing Ltd

where $\boldsymbol{p}$ is the momentum operator, $\boldsymbol{\sigma}$ is Pauli matrices with $\boldsymbol{\sigma} = (\sigma_x, \sigma_y)$, $\upsilon_{\rm F}$ is the Fermi velocity, and γ_0 and x_0 are the doping potential parameter and the doping position parameter, respectively. The system presented can be separated into three regions by the magnetic tunnel junction as I ($x < 0$), Ⅱ ($0 < x < D$), and Ⅲ ($x > D$). We introduce the dimensionless units: $\boldsymbol{r} \to \ell_B \boldsymbol{r}$, $E \to EE_0$, $B(x) \to B_0 B(x)$, $A(x) \to B_0 \ell_B A(x)$,$\gamma_0 \to \gamma E_0 \ell_B$ and $E_0 = \hbar \upsilon_{\rm F}/\ell_B$. In these units, Eq. (1) is explicitly written as

$$H = -i \begin{pmatrix} 0 & \partial_x - i\partial_y + B \\ \partial_x + i\partial_y - B & 0 \end{pmatrix} + \gamma\delta(x - x_0). \tag{2}$$

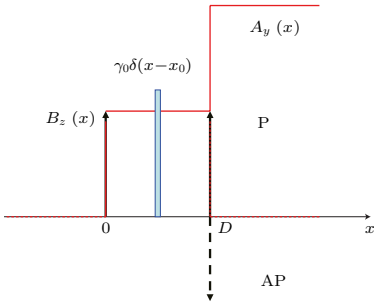

Fig. 1. Schematic diagram of the magnetic profile as well as a δ doping in the GMTJ device, where the black solid arrows and black dashed arrows correspond to the direction of magnetic field in parallel (P) and in antiparallel (AP) with the configuration, respectively. The red solid and the red dashed lines correspond to the magnetic vector potential for the P and AP configurations, respectively.

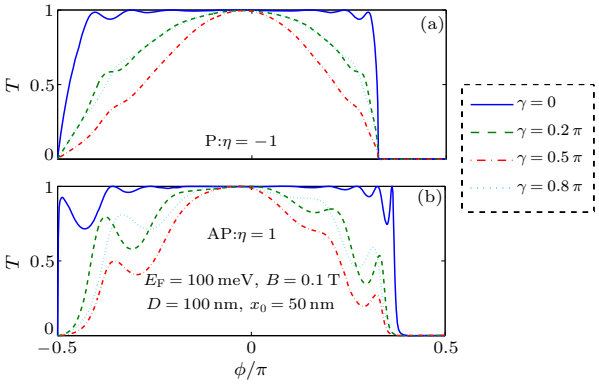

Fig. 2. Variation of the transmission probability with the angle of the incident electron ϕ for (a) the P configuration and (b) the AP configuration, where the δ-doping potential parameter γ is chosen as $\gamma = 0$, 0.2π, 0.5π and 0.8π. The values of the other parameters are $D = 100$ nm, $E_{\rm F} = 100$ meV, $x_0 = 50$ nm and $B = 0.1$ T.

In the left region of this nanostructure, the wavefunction can be written as

$$\psi(x) = \frac{1}{\sqrt{2}} \begin{pmatrix} 1 \\ e^{i\phi} \end{pmatrix} e^{ik_{\rm l}x} + \frac{r}{\sqrt{2}} \begin{pmatrix} 1 \\ e^{i(\pi-\phi)} \end{pmatrix} e^{-ik_{\rm l}x},$$

where $\phi = \arctan(k_y/k_{\rm l})$, $k_{\rm l} = k_{\rm F}\cos(\phi)$, and $k_y = k_{\rm F}\sin(\phi)$. In the right region, we have a transmitted wave only

$$\psi(x) = \frac{t}{\sqrt{2}} \begin{pmatrix} 1 \\ e^{i\theta} \end{pmatrix} e^{ik_{\rm r}x},$$

where $\theta = \arctan(q_y/k_{\rm r})$, $k_{\rm r} = \sqrt{k_{\rm F}^2 - q_y^2}$, and $q_y = k_y + B - \eta B$. Thus the transmission probability for electrons through the nanostructure can be obtained by using the wavefunction in boundaries[30] as $T(E, k_y) = \frac{\cos(\theta)}{\cos(\phi)}|t|^2$. With the transmission probability, in the liner transport regime at zero temperature, the conductance G can be calculated from the well-known Landauer–Buttiker formula[27,29−31]

$$G = G_0 \int_{-\pi/2}^{\pi/2} T(E_{\rm F}, B, E_{\rm F}\sin(\phi), \gamma, x_0)\cos(\phi)d\phi, \tag{3}$$

where $G_0 = e^2 E_{\rm F} W/(\pi^2\hbar^2\upsilon_{\rm F})$, W is the length of the structure along the y-direction, and $E_{\rm F}$ is the Fermi energy.

In the following, the typical width of the GMTJ device $D = 100$ nm and the Fermi energy $E_{\rm F} = 100$ meV are chosen to discuss the transmission probability and conductance. The transmission probability is rather complicated while we note that it contains the doping parameter γ only in the form of $\cos^2(\gamma)$ and $\sin(2\gamma)$, that is, $T(\gamma + \pi) = T(\gamma)$ is always satisfied. In view of the above facts, we can choose the value of γ from 0 to π in the following.

Figure 2 exhibits the transmission probability as a function of the angle ϕ for several values γ. The result shows that the transmission probability has an oscillation with the variation of the angle of the incident electron ϕ in the P and AP configurations. Obviously, transmission probability is no longer symmetric with the sign of the incident angle. Even when the incident angle attains a certain value, the transmission probability is totally suppressed. This characteristic occurring in the AP configuration is more obvious than that occurring in the P configuration. Obviously, the number of the modes in the AP configuration is more than that in the P configuration. For the AP configuration, the allowed incident angle ϕ is $-1 \le \sin(\phi) \le 1 - B/k_{\rm F}$, while for the P configuration the allowed incident angle ϕ is $-1 \le \sin(\phi) \le 1 - 2B/k_{\rm F}$. For the AP configuration, as the incident angle is more than a certain value $\phi_{\rm c} \equiv \arcsin(1 - B/k_{\rm F})$, the transport through the GMTJ can only be maintained by evanescent waves. However, for the P configuration, the value of $k_{\rm r}$ in the right region, $k_{\rm r} = \sqrt{k_{\rm F}^2 - (k_y + 2B)^2}$, is imaginary when the incident angle is more than a certain value $\phi_{\rm c} \equiv \arcsin(1 - 2B/k_{\rm F})$, thus in the right region the transmitted wave is suppressed. In addition, with increasing the doping potential parameter γ, the result shows characteristic oscillations of the resonant tunneling structures.

Figure 3 displays the transmission probability as a function of the angle ϕ for the P configuration (Fig. 3(a)) and the AP configuration (Fig. 3(b)), where x_0 is chosen as $x_0 = 0$, 25, 50 and 100 nm. Obviously, the result also shows characteristic oscillations of the resonant tunneling structures due to the fact that the dependence of x_0 on the phase factor of transmission coefficient t always retains the term: $\exp(\pm 2iqx_0)$,

where $q = \sqrt{k_F^2 - (k_y + B)^2}$. For the AP configuration, it is easily found that the transmission probability is with the form $T(x_0) = T(D - x_0)$ due to the symmetry of the profile of the magnetic vector potential. Obviously, this distinguishes the result from the P configuration. In both cases, the doping position parameter can also dramatically change the transmission probability, especially for the large ϕ. In addition, the position parameter can shift the peak of the transmission probability to the left. Obviously, the number of the propagating modes in the AP configuration is more than that in the P configuration. If we define MR=$(G_{AP} - G_P)/G_{AP} \times 100\%$, the MR effect can be modulated by controlling the position parameter γ or potential parameter x_0.

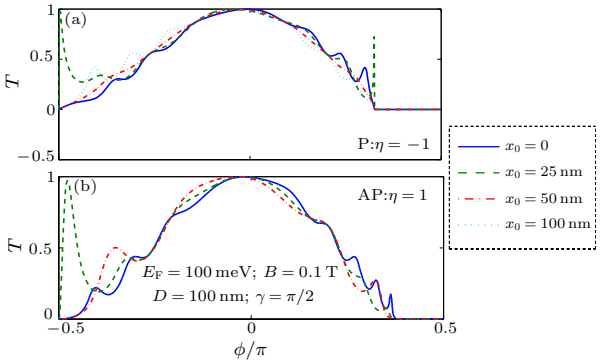

Fig. 3. Variation of the transmission probability with the angle of the incident electron ϕ for (a) the P configuration and (b) the AP configuration, where the δ-doping position parameter x_0 is chosen as $x_0 = 0$, 25, 50 and 100 nm. The values of the other parameters are set as $D = 100$ nm, $E_F = 100$ meV, $\gamma = \pi/2$ nm and $B = 0.1$ T.

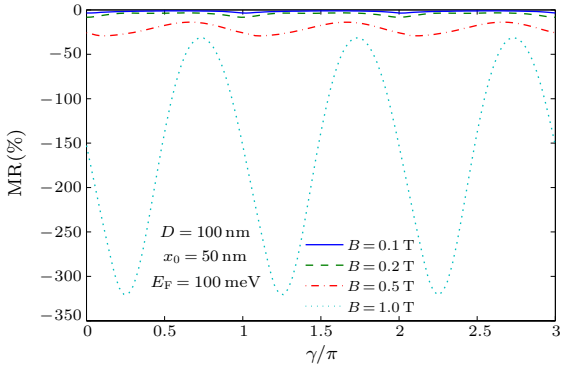

Fig. 4. Schematic diagram of the MR as a function of the δ-doping potential parameter γ for the fixed magnetic field $B = 0.1$, 0.2, 0.5 and 1.0 T. The other physical parameters are set as $D = 100$ nm, $E_F = 100$ meV and $x_0 = 50$ nm.

Figure 4 shows the MR as a function of γ for several values of B. The MR produces a π-periodic oscillation with γ. Furthermore, the MR is always negative and a large negative value of the MR can be obtained by the modulation magnetic field. The reason is that the number of the propagating modes in the AP configuration is more than that in the P configuration. For a narrow conductor each propagating mode independently contributes to conductance, that is, $G \sim \frac{4e^2}{h} MT$, where M is the number of propagating modes.[31,32] From the above analysis, we know that the magnetic field can suppress the propagating modes in both cases, while this characteristic in the P configuration is more obvious than that in the AP configuration. With the increase of B, the propagating modes rapidly reduced in the two cases, which leads to the dramatic change of the conductance. As we can see in Fig. 5, the absolute value of the MR is over 300% as the magnetic field is set as $B = 1.0$ T.

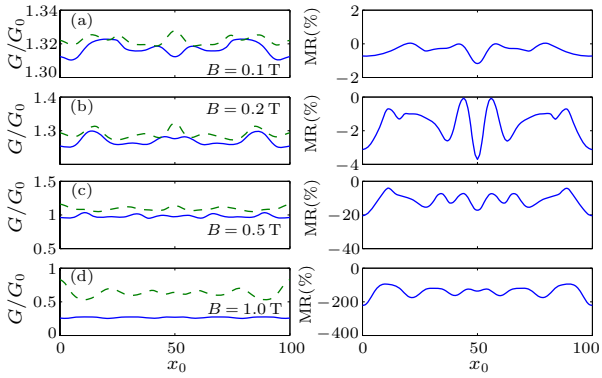

Fig. 5. Schematic diagram of the conductance (left panel) and the MR (right panel) as a function of the δ-doping position parameter x_0 for the fixed magnetic field (a) $B = 0.1$ T, (b) $B = 0.2$ T, (c) $B = 0.5$ T and (d) $B = 1.0$ T, respectively. The other physical parameters are set as $D = 100$ nm, $E_F = 100$ meV and $\gamma = \pi/2$. The solid and dashed lines correspond to the P configuration and the AP configuration, respectively.

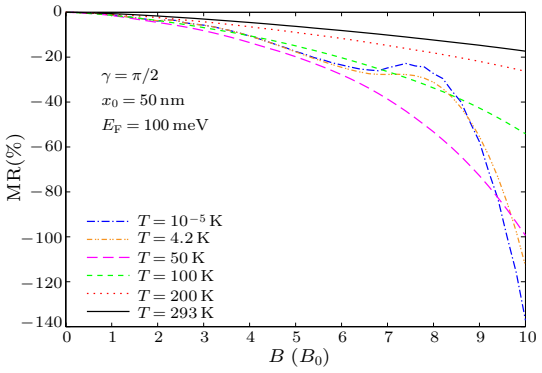

Fig. 6. Schematic diagram of the MR as a function of the magnetic field B. The other physical parameters are set as $D = 100$ nm, $E_F = 100$ meV, $x_0 = 50$ nm and $\gamma = \pi/2$.

Figure 5 depicts the conductance (left panel) and the MR (right panel) as a function of x_0 for several values of B. The magnetic field can suppress dramatically the propagating modes in both cases, especially for the P configuration. As a result, the conductance for the P configuration is always less than that for the AP configuration. With the increase of B, the conductance spacing between the two cases is becoming larger and larger, thus one can use a large value B to obtain the large MR. We find that the position parameter x_0 can cause the characteristic oscillations of the conductance (left panel) and MR (right panel) due to the position parameter x_0 dependence of the phase interference. From Fig. 5, the conductance (left panel) and MR (right panel) are symmetric with re-

spect to $x_0 = D/2$. For the AP configuration, the transmission probability is symmetric with respect to $x_0 = D/2$, while the transmission probability is no longer symmetric with respect to $x_0 = D/2$ in the P configuration (see Fig. 3). We need to declare that the electron passes through the GMTJ device from left to right in the process of the above discussion. In the three regions of the device, the effective transverse wave vectors can be written as $\tilde{k}_y = k_y$, $k_y + B$ and $k_y + 2B$ corresponding to the left, middle and right regions, respectively. The conductance can be written as $G(x_0) = \frac{4e^2}{h}\frac{W}{2\pi}\int T(k_y, x_0)dk_y$, where the allowed transverse wave vectors dependence of the propagating modes satisfies the form $-k_{\rm F} \leq k_y \leq k_{\rm F} - 2B$ for using the dimensionless units. If we think that the electron passes through the GMTJ device from right to left, the effective transverse wave vectors can be written as $\tilde{k}_y = q_y$, $q_y - B$ and $q_y - 2B$ corresponding to the right, middle and left regions, respectively. The conductance can be written as $G(D - x_0) = \frac{4e^2}{h}\frac{W}{2\pi}\int T(q_y, D - x_0)dq_y$, where the allowed transverse wave vector dependence of the propagating modes satisfies the form $-k_{\rm F} + 2B \leq q_y \leq k_{\rm F}$. Obviously, $G(x_0) \equiv G(D - x_0)$, that is, the conductance is also symmetric with respect to $x_0 = D/2$ in the P configuration. Thus it is easy to understand why the conductance and the MR are symmetric with respect to $x_0 = D/2$. To generalize our results to nonzero temperature, we can replace the function of $G = G(E_{\rm F})$, which depends on the Fermi energy $E_{\rm F}$ by the corresponding average over the derivative of the Fermi function[31] $G = G(E_{\rm F}) = \int G(E)(-\frac{\partial f_0}{\partial E})dE$, where $f_0 = \frac{1}{\exp[(E-E_{\rm F})/k_{\rm B}T]+1}$. Figure 6 shows the MR as a function of the magnetic field B at six different temperatures. As the temperature increases, the MR drastically decreases and the quantum effect disappears. Also the finite temperatures smooth the zero-temperature results.

In summary, we have theoretically investigated the tunneling magnetoresistance via the δ doping in a graphene-based magnetic tunnel junction in detail. The results show that the transmission probability and the conductance oscillate with the position and the aptitude of the δ doping. Also, both the transmission probability and the conductance at the parallel configuration are suppressed by the magnetic field more obviously than that at the antiparallel configuration, which implies a large negative magnetoresistance for this device when the large magnetic field is applied. The results show that the negative magnetoresistance of over 300% at B=1.0 T is observed by choosing suitable doped parameters and the temperature plays an important role in the magnetoresistance. Thus it is possible to open a way to effectively manipulate the magnetoresistance devices, and to make a type of magnetoresistance device by controlling the structural parameter of the δ doping.

References

[1] Novoselov K S, Geim A K, Morozov S V et al 2004 *Science* **306** 666
[2] Castro Neto A H, Guinea F, Peres N M R, Novoselov K S and Geim A K 2009 *Rev. Mod. Phys.* **81** 109
[3] Kim K S, Zhao Y et al 2009 *Nature* **457** 706
[4] Li X, Cai W, An J et al 2009 *Science* **324** 1312
[5] Friedman A L, Robinson J T, Perkins F K and Campbell P M 2011 *Appl. Phys. Lett.* **99** 022108
[6] Xu H, Heinzel T, Evaldsson M and Zozoulenko I V 2008 *Phys. Rev.* B **77** 245401
[7] Masir M R, Vasilopoulos P and Peeters F M 2010 *Phys. Rev.* B **82** 115417
[8] Guo Y Y and Guo Y 2009 *J. Appl. Phys.* **105** 063717
[9] Zhai F and Chang K 2008 *Phys. Rev.* B **77** 113409
[10] Masir M R, Vasilopoulos P and Peeters F M 2009 *New J. Phys.* **11** 095009
[11] Tan L Z, Park C H and Louie S G 2010 *Phys. Rev.* B **81** 195426
[12] Park C H, Yang L, Son Y W, Cohen M L and Louie S G 2008 *Nat. Phys.* **4** 213
[13] Biswas R, Biswas A, Hui N and Sinha C 2010 *J. Appl. Phys.* **108** 043708
[14] Luca D A and Alessandro D M 2009 *Phys. Rev.* B **79** 045420
[15] Friedman A L, Erve O M J, Robinson J T, WhitenerK E and Jonker B T2015 *ACS Nano* **9** 6747
[16] Erve O M J, Friedman A L, Li C H, Robinson J T, Connell J, Lauhon L J and Jonker B T 2015 *Nat. Commun.* **6** 7541
[17] Friedman A L, Erve O M J, Li C H, Robinson J T and Jonker B T 2014 *Nat. Commun.* **5** 3161
[18] Cobas E, Friedman A L, Erve O M J, Robinson J T and Jonker B T 2013 *IEEE Trans. Magn.* **49** 4343
[19] Friedman A L, Tedesco J L, Campbell P M et al 2010 *Nano Lett.* **10** 3962
[20] Matis B R, Bulat F A, Friedman A L, Houston B H and Baldwin J W 2012 *Phys. Rev.* B **85** 195437
[21] Cerchez M, Hugger S, Heinzel T and Schulz N 2007 *Phys. Rev.* B **75** 035341
[22] Matulis A, Peeters F M and Vasilopoulos P 1994 *Phys. Rev. Lett.* **72** 1518
[23] Xu H Z and Shi Z 2004 *Phys. Rev.* B **69** 237201
[24] Lu J D 2009 *Appl. Surf. Sci.* **255** 7348
[25] Lu J D, Xu B, Liu H Y and Dai H M 2014 *Phys. Lett.* A **378** 286
[26] Myoung N and Ihm G 2011 *J. Appl. Phys.* **109** 053716
[27] Ghosh S and Sharma M 2009 *J. Phys.: Condens. Matter* **21** 292204
[28] Ghosh S and Sharma M 2011 *J. Phys.: Condens. Matter* **23** 055501
[29] Yuan J H, Zhang J J, Zeng Q J, Zhang J P and Cheng Z 2011 *Physica* B **406** 4214
[30] Yuan J H, Zhang Y, Guo X, Zhang J and Mo H 2015 *Solid State Commun.* **206** 31
[31] Datta S 1997 *Electronic Transport in Mesoscopic Systems* (Cambridge: Cambridge University Press)
[32] van Wees B J, van Houten H, Beenakker C W J, Williamson J G, Kouwenhoven L P, van der Marel D and Foxon C T 1988 *Phys. Rev. Lett.* **60** 848